ISSN : 0974 - 746X Volume 11 Issue 1

Inorganic CHEMISTRY

An Indian Journal

Full Paper

ICAIJ, 11(1), 2016 [001-009]

Kinetic study of nickel hydroxide thermal decomposition by constant rate thermal analysis (CRTA) at 5hPa water vapor pressure

Raoudha Yahyaoui, Kais Nahdi*

Laboratoire d'Application de la Chimie aux Ressources et Substances Naturelles et à l'Environnement, Faculté des Sciences de Bizerte, université de carthage, 7021 Zarzouna, Bizerte, (TUNISIE)

E-mail: k_nahdi@yahoo.fr

ABSTRACT

The kinetic study of $Ni(OH)_2$ dehydroxylation was carried out by means of constant rate thermal analysis technique in the temperature range from 248K up to 873K and at controlled residual water vapour pressure equal to 5 hPa. Apparent activation energy was measured experimentally, without any assumption on the kinetic model, using two CRTA curves carried out at two constant rates in the ratio C2:C1=3. The linear regression method was applied to estimate the conversion function f(α).

KEYWORDS

Nickel hydroxide;
Thermal decomposition;
Activation energy;
Kinetic;
CRTA.

INTRODUCTION

Hydroxides with general formula $M^{II}(OH)_2$ (M^{II}: bivalent metal element) derive their structures from that of mineral brucite, Mg(OH)2. Nickel hydroxide exists in two allotropic phases: β-$Ni(OH)_2$ and α-$Ni(OH)_2$. While the β phase is isostructural with $Mg(OH)_2$, in the α phase, a fraction, x, of the hydroxyl ions are protonated leading to positively charged layers of the composition $[M(OH)_{2-x}(H_2O)_x]^{x+}$. The deficit in charge is balanced by the incorporation, in the interlayer region, of anions and water molecules which leads to the increase of the interlayer spacing (c/3 = 7.6 Å when the anion is CO_3^{2-})[1].

Nickel hydroxide material is used as a positive electrode material in all Ni-based alkaline secondary cells[2], as an active material in electrochromic devices, supercapacitors, and as a precursor for catalysts[3-7]. Its thermal decomposition product (NiO) is a semiconductor and an antiferromagnetic material. It can be used as catalysis[8,9], battery cathode[10,11], gas sensors[12,13], electrochromic films[14,15], active optical fibers[16] and fuel cell electrodes[17,18].

The thermal decomposition of $Ni(OH)_2$ to synthesize NiO has been widely studied[19-28]. The role of preparative conditions on the thermal decomposition and its influence on the changes on the powder X-ray diffraction pattern have been reported[21,22].

The synthesis of porous microspheres, nanobelts, nanowires, nanoplates, nanosheets, and nanocolumn blocks has been described for nickel oxide materials[23–26]. The materials such as ordered mesoporous NiO with thick crystalline walls and a bimodal pore size[27] and coralloid nanostructured NiO[28] are available now.

Concerning the kinetic study of nickel hydroxide thermal decomposition, only few works exist[29-

Full Paper

TABLE 1 : Literature data for the decomposition kinetics of $Ni(OH)_2$

References	TG technique	Atmosphere	Kinetic law	Ea/ kJ.mol^{-1}
[29]	Non isotherm	vacuum	R2 (0.1<α<0.6)	97
		Air	R2 (0.1<α<0.6)	89
[30]	Non isotherm	He	Fn or CnB (0.15<α<0.80)	101
[31]	Isotherm	Air	(m/m0)0.33=kt+1	119
[32]	Isotherm	air	An	177

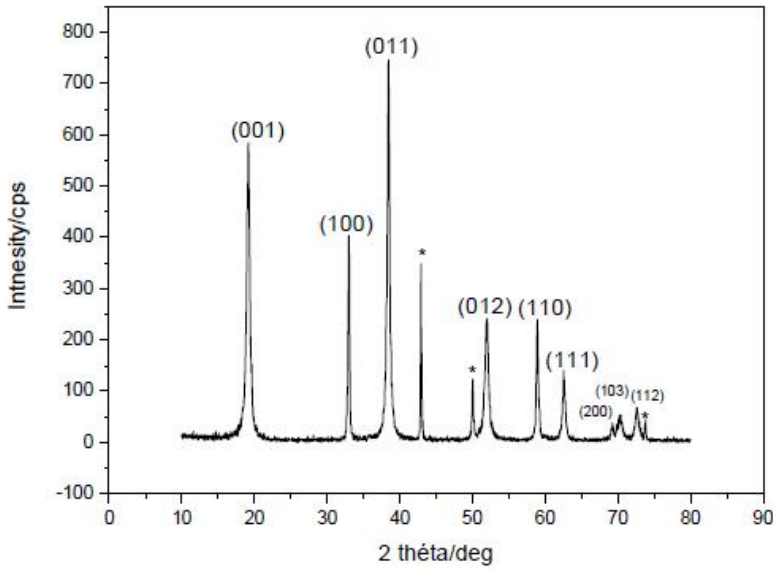

Figure 1 : XRD pattern of $Ni(OH)_2$

[32]. The experimental conditions and the main resultants of these works are mentioned in TABLE 1.

As can be seen, the kinetic of thermal decomposition of $Ni(OH)_2$ depends strongly on the experimental conditions such as atmosphere above the sample, nature of thermal treatment and temperature of the isotherm, which made it difficult to compare results from different authors.

Although the dehydroxylation reaction of nickel hydroxide (R.1) seems simple, there is no agreement on the appropriate kinetic parameters.

$Ni(OH)_2(sd) = NiO(sd) + H_2O(g)$ (R.1)

In any case it makes sense to try to carefully control the pressure of gas product during the whole experiment and not only above but also within the sample. This can be achieved by using constant rate thermal analysis (CRTA) technique[33]. This technique has been employed with success in the investigation of the kinetic parameters of kaolinte[34], brucite[35], cerium cyclophosphate[36] and neodymium cyclophosphate[37].

The present work is the first kinetic study of $Ni(OH)_2$ dehydroxylation carried out by Constant Rate Thermal Analysis technique. Its aim is to contribute to the kinetic study of nickel hydroxide thermal decomposition under controlled and low residual water vapor pressure (5 hPa). As pointed out by Galwey in his comprehensive survey of the thermal dehydration of crystalline solids[38], only measurements with a very careful control of the experimental conditions (and specially of the water pressure) can be expected to bring a new and concrete knowledge in this field. This is what we aim to achieve with the help of CRTA.

EXPERIMENTAL AND METHODS

Sample

The sample under investigation, $Ni(OH)_2$, was commercially obtained from Across (lot A017490201). Its X-ray diffraction pattern (Figure 1) shows sharp peaks at 4.63 Å, 2.71 Å, 2.28 Å, 1.75 Å, 1.56 Å, 1.48 Å, 1.35 Å, 1.33 Å and 1.29Å

which are respectively attributed to (001), (100), (011), (012), (110) (111), (200), (103) and (112) plane of a well crystallized Ni(OH)2 [JCPDS 73-1520]. The essential impurity present in the studied sample is nickel oxide (reûections at 2.10 Å, 1.82 Å and 1.26Å).

Techniques

TG and DSC measurement were operated by heating the sample under air atmosphere at a rate of 10 K.min^{-1}. The used equipment is a TGA/DSC1 star system power 400w. Sample was analyzed at a heating rate of 10 K.min^{-1} in air. The sample mass in the aluminous pan was kept at about 42.7 mg. The reference pan was pure aluminum pan. The temperature and energy of instrument had been calibrated by standard metal In, before all measurements. Powder X-ray diffraction measurements (XRD) were recorded using a Bruker X-ray diffraction unit Cu Kα radiation (λ = 1.5406 Å) at room temperature in 40 kV and 30 mA at a scan speed of 1.2°min^{-1}. The infrared absorption spectra of a KBr pressed pellet of the powdered samples were studied in the range 4000-400 cm^{-1} using a brucker alpha type spectrophotometer. The Constant Rate Thermal Analysis (CRTA) experiments were carried out on an apparatus built in house and 100mg samples weighed in a silica-cell in the temperature range from 248K up to 873K. Once the equilibrium temperature is reached, the pressure above the sample is lowered using vacuum pumping system from 1 bar to the desired value (5hPa in our case). The pressure is continuously followed using a Pirani gauge (PID control) placed in proximity of the sample. The pressure signal produced by the Pirani gauge is sent to the furnace-heating controller. The heating of the sample then takes place in such a way as to keep constant, at the preset value, the vapour pressure generated by the sample[39].

RESULTS AND DISCUSSION

Thermal behavior in air by TG-DTG and DSC

Figure 2 and Figure 3 show, respectively, the TG-DTG and DSC curves of the starting material. The TG curve exhibits a total mass loss equal to 20.67 % attributed to the complete dehydroxylation of $Ni(OH)_2$. The excess of mass loss (1.26%) can be attributed to the residual adsorbed water. The DTG curve shows one intense peak centered at 581 K which is close to the endothermic peaks observed in the DSC curve at 583 K.

To identify each thermal phenomena observed in TG and DSC curves, XRD and IR techniques were applied to samples of $Ni(OH)_2$ partially decomposed by heating in an electric furnace in air at 435 K, 573 K, 673 K, 723 K and 873 K. The corresponding X-ray diffraction patterns and IR spectra are shown in Figure 4 and Figure 5 respectively.

Up to 573 K temperature heating, the X-ray patterns are similar to that of the starting sample. After

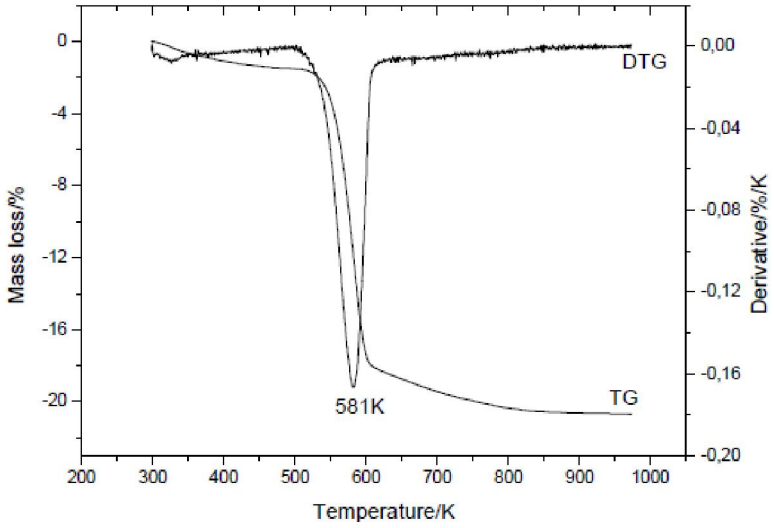

Figure 2 : TG–DTG curves of $Ni(OH)_2$ in air

Full Paper

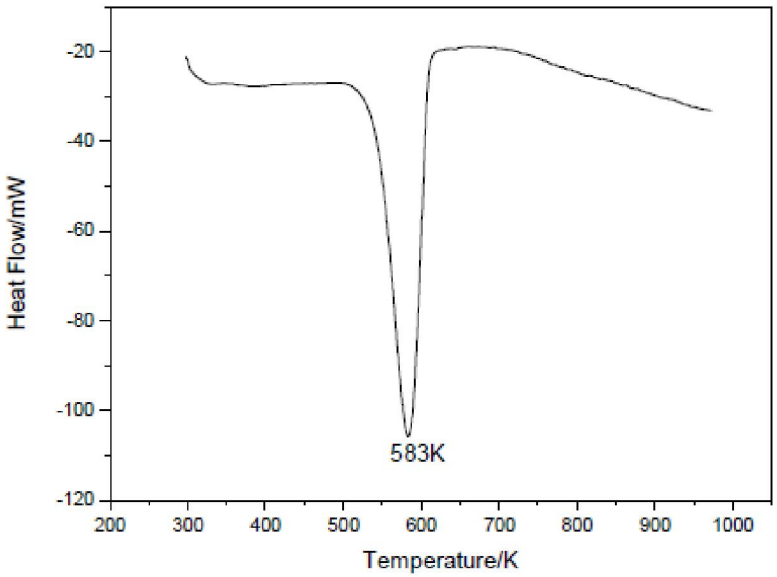

Figure 3: DSC curve of of $Ni(OH)_2$ in air

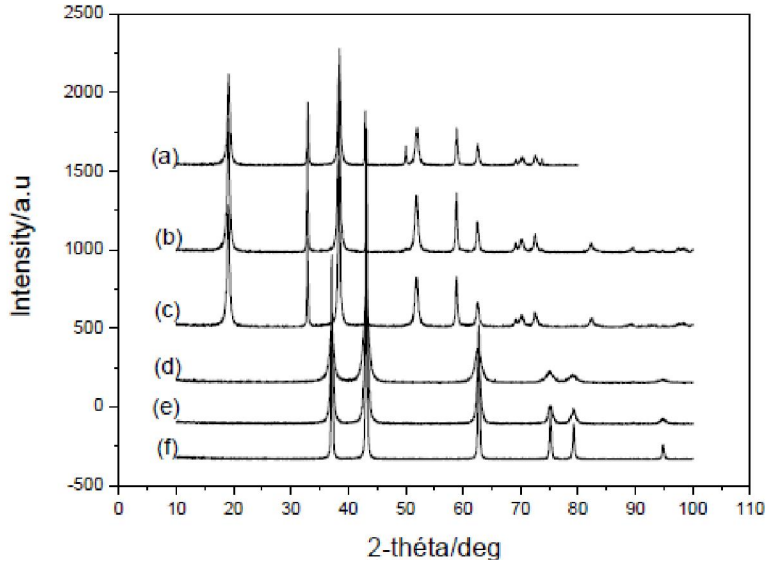

Figure 4 : XRD patterns of the initial material (a) and of intermediate products obtained at 435K (b) 573K (c) 673K (d) 723K (e) and 873K (f) in air

calcination at 673K all reflections due to $Ni(OH)_2$ disappear completely and those corresponding to cubic NiO phase appear and increase in intensity up to 873K of heating temperature. The disparition of the characteristic absorption band of OH- (centered at 3645cm^{-1}) in the IR spectra at 673K, is in accord with the above result. Thus $Ni(OH)_2$ dehydroxylation is totally acheived at 673K and can be described by reaction (R.1).

Thermal behavior by CRTA technique at P_{H2O} =5 hPa

The CRTA curves of $Ni(OH)_2$ thermal decomposition, shown in Figure 6, were obtained by thermolysis of 100 mg of sample under 5 hPa partial pressure from 248 to 873 K. The final mass loss at 873 K is 20.43% which corresponds to the theoretical loss (19.41%) of one water molecule. The CRTA curves show the sample temperature (curve I) variation with time, controlled so as to keep constant the pressure (curve II) above the sample. Here, we have considered that, under 5 hPa, dehydroxylation starts at 446 K which is the temperature at which the constant pressure regime, required for CRTA, is reached. At around 852 K, a rapid drop in the pressure signal is observed indicating the end of the dehydroxyaltion

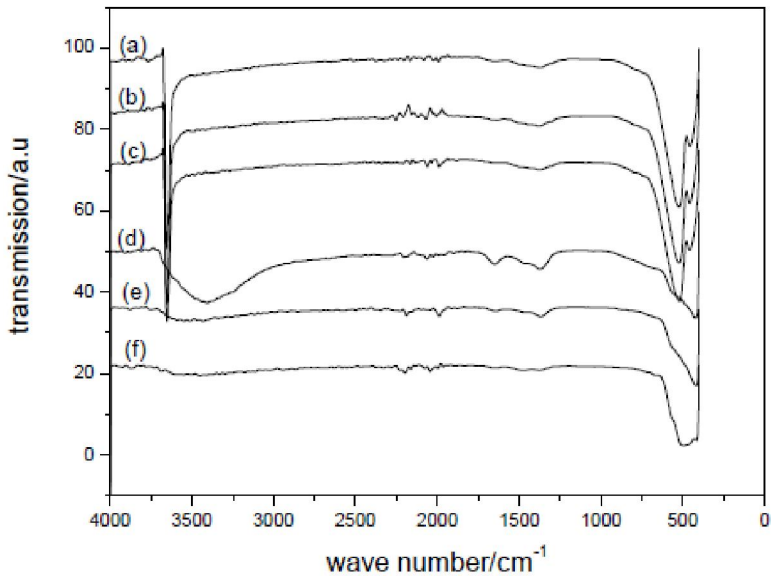

Figure 5 : IR spectra of the initial material (a) and of intermediate products obtained at 435K (b) 573K (c) 673K (d) 723K (e) and 873K (f) in air

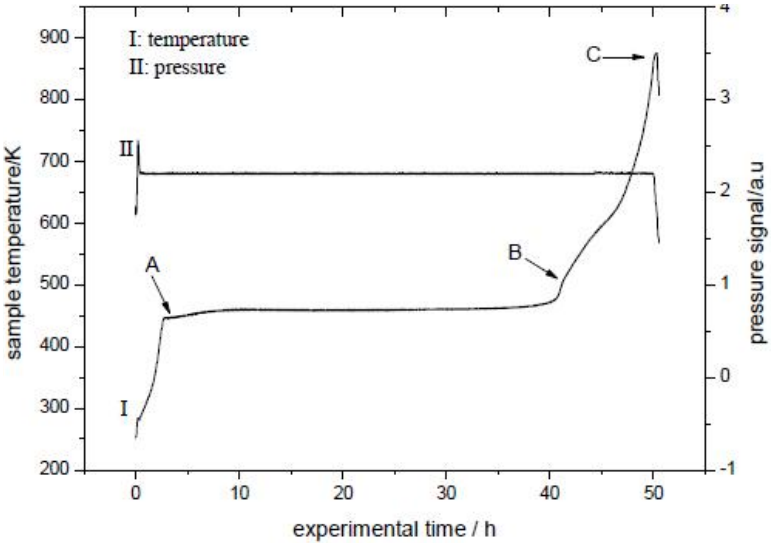

Figure 6 : Experimental CRTA curves for dehydroxylation of $Ni(OH)_2$ at P_{H2O} = 5 hPa

of the initial phase. The total thermolysis occurs within 50 hours which corresponds to a rate of thermal decomposition equal to 0.4086 $mg.h^{-1}$. Based on the changes in the slope of the temperature curve and the change in the pressure signal, it is possible to consider two decomposition steps. The first step (A-B) occurs within 40 hours in the temperature range 446K - 490K and the second stage (B-C) takes place within 10 hours between 490K and 852K.

The residue from thermolysis of $Ni(OH)_2$ by CRTA at 873K was analyzed by X-ray diffraction (Figure 7) and by infrared spectroscopy (Figure 8). The obtained phase at the end of the reaction is a pure NiO. Thus dehydroxyaltion of $Ni(OH)_2$ in CRTA conditions is total and can be described by reaction (R.1).

Now it is possible to describe the CRTA curve (temperature vs time) and to delimit the $Ni(OH)_2$ dehydroxylation domain. However, the mass loss before point A corresponds to the release of adsorbed water, in the range (A–B) takes place the dehydroxylation of $Ni(OH)_2$ and the range (B–C) corresponds to the release of the remained hydroxyl group in the intial phase and the formation of pure NiO cubic phase. Thus, the experimental CRTA curve (temperature vs time) may be converted into plots

Full Paper

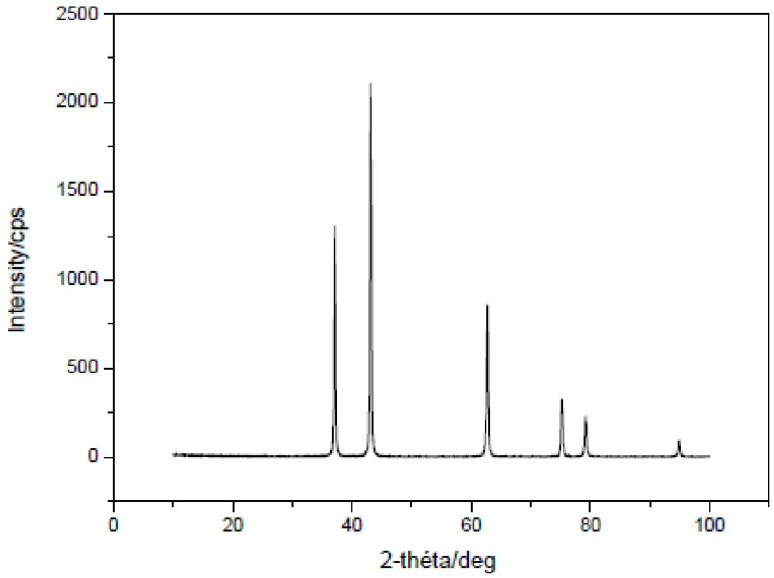

Figure 7 : XRD pattern of $Ni(OH)_2$ decomposed by CRTA up to 873K

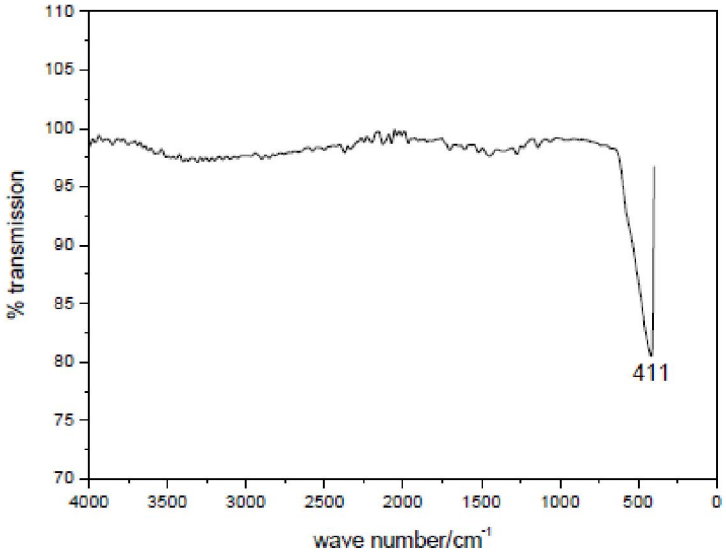

Figure 8 : IR spectrum of $Ni(OH)_2$ decomposed by CRTA up to 873K

of degree of advancement α vs temperature, (where α = t/Δt, Δt being the total duration of dehydroxylation).

Kinetic of dehydroxylation by CRTA

Theory

In heterogeneous kinetics, in the simplest cases, the rate law is assumed to be expressed by the product of two terms: the change of the advancement degree of reaction α vs time which can be described with the help of mathematical functions f(α) like those listed by sharp and al.[40] for a number of limiting cases. The second term depends only on temperature and pressure. If the Arrhenius law is obeyed, the rate law can be written:

$$\frac{d\alpha}{dt} = Aa \times f(\alpha) \times \exp\left[\frac{-Ea}{RT}\right] \quad (1)$$

Where Aa is the apparent pre-exponential factor and Ea is the apparent Arrhenius activation energy.

Since the above experiment is carried out in isokinetic condition, we can state:

$$\frac{d\alpha}{dt} = constant = C \quad (2)$$

When using CRTA, a first idea of the kinetic law involved is easily obtained by comparing the experimental curves α vs T with the set of isokinetic theoretical curves built by Criado and al.[41] and which

easily split into three groups, on the basis of their general shape (Figure 9).

Process F1 corresponds to the case when the transformation rate of each single particle, is limited by a random nucleation, itself followed by a very rapid growth of the nuclei. Processes R2 and R3 correspond to an interfacial reaction. Processes D1, D2, D3, and D4 correspond to the case when the transformation rate is limited by diffusion through the layer of solid product and processes A2 and A3 correspond to nucleation and nuclei growth.

Experimental results

Here the kinetic study concerns the measure of the apparent activation energy and the determination of the most probable f(α) function for $Ni(OH)_2$ dehydroxylation.

α_{AC}, α_{AB} and α_{BC} are the degree of advancement of reaction associated to (A-C), (A-B) and (B-C) steps respectively.

Activation energy measurement

The experimental activation energy Ea of a reaction can be obtained directly during a single rate jump experiment using a setup described elsewhere[42] where the reaction rate changes between two values with periodical use of a second diaphragm (assessed by means of an automated vacuum valve) allowing to operate at two alternate pumping rates. Thus for a single value of α during a reaction, without any presumption of the reaction mechanism and whilst keeping all other parameters identical (sample mass, residual pressure) an expression of the activation energy, at a given value of α, can be obtained:

$$Ea = \frac{R \times T_1 \times T_2}{T_2 - T_1} ln\left[\frac{C_2}{C_1}\right] \quad (3)$$

where T_1 and T_2 are the temperatures corresponding to the rates C_1 and C_2.

In our study, the activation energies were measured using two CRTA curves obtained under the same residual water vapor pressure (5hPa) and at two different rates in the ratio C2:C1 = 3. Here again, temperatures can be evaluated for the same value of α and then an activation energy is deduced using equation (3).

In Figure 10 are reported the different values of Ea as a function of the degree of advancement of reaction "α_{AC}". The apparent activation energies measured can be considered as constant up to α_{AC} = 0.80 with a main value equal to 286±10kJ.mol^{-1}.

Estimation of the conversion function f(α)

The kinetic analysis consists of following the change of ln[f(α)] as a function of 1/T, which varies in a linear manner when the chosen function f(α) corresponds to the most probable single elementary process. The comparison of the activation energy determined from the slope of the line obtained via this latter method with the experimentally measured value adds a supplementary criterion to the elementary process.

Since the apparent Arrhenius activation energies measured are constant, only for α_{AC} up to 0.80 i.e. for temperature up to 490 K (point B), it is possible to consider that a process characterized by the measured activation energy ends at this point. So, plot of ln[f(α_{AB})] vs 1/T for each f(α) functions listed by Sharp can be carried out.

In TABLE 2 are given, the linear regression coefficient r^2, the apparent activation energy Ea and the apparent pre-exponential factor Aa for each kinetic law.

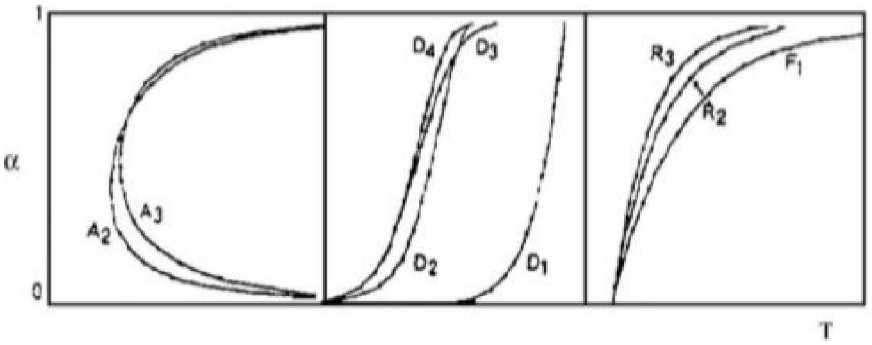

Figure 9 : Theoritecal α vs T kinetic curves as obtained with the assumption of CRTA

Full Paper

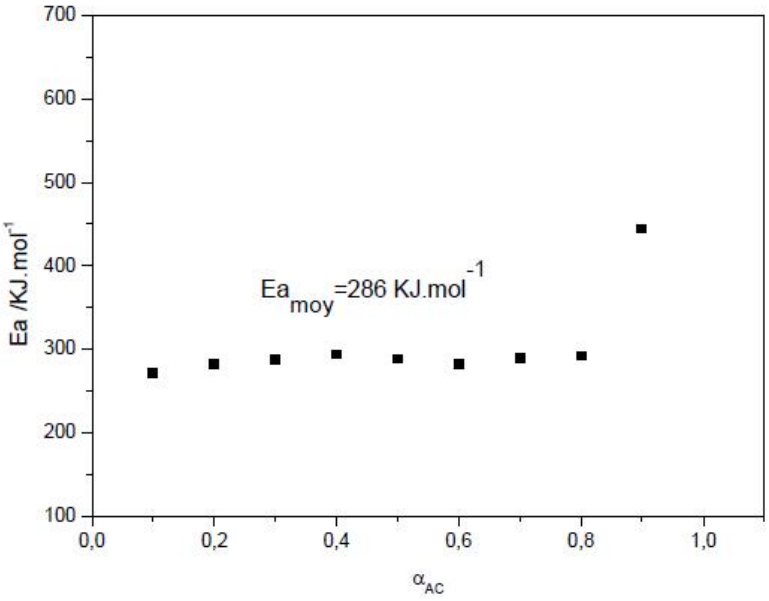

Figure 10 : Variation of the activation energy as a function of αAC at PH2O = 5hPa

TABLE 2 : Linear regression coefûcients r^2 and Arrhenius parameters obtained for kinetic laws applied to the experimental CRTA curve in the range $0 \leq \alpha_{AC} \leq 0.8$

Kinetic law	Ea/kJ.mol^{-1}	A /s^{-1}	r^2
F1	438	5.4x10^{27}	0.939
R_2	219	4,0x10^{27}	0.939
R_3	292	1,9x10^{28}	0.939
D_1	189	2.6x10^{27}	0.406
D_2	338	1.7x10^{27}	0.564
D_3	355	2,1x10^{27}	0.826
D_4	420	2.0x10^{27}	0.629
A_2	269	3.5x10^{27}	0.902
A_3	213	2.6x10^{27}	0.726

It can be seen that the F1, R2, R3 and A2 kinetics laws give the highest values of linear regression coefficient. However, the kinetic law of three-dimensional advance of reaction interface (R3) gives the nearest activation energy (292 kJ.mol^{-1}) to the one measured experimentally (286 kJ.mol^{-1}).

Based on the Ea value measured experimentally R3 law seems to be the most probable kinetic law for the dehydroxylation of $Ni(OH)_2$.

CONCLUSION

This work, concerns the kinetic study of $Ni(OH)_2$ thermal decomposition carried out by constant rate thermal analysis technique at 5hPa of residual water vapour pressure. The rate of thermal decomposition is equal to 0.3886 mg.h^{-1}. It was shown that dehydroxylation occurs according to the three-dimensional advance of reaction interface (R3) with apparent activation energy equal to 286 kJ.mol^{-1}.

REFERENCES

[1] P.V.Kamath, G.H.A.Therese, J.Gopalakrishnan; J.Solid.State.Chem., **128**, 38 **(1997)**.
[2] S.U.Falk, A.J.Salkind, Alkaline Storge Batteries; Wiley: New York, **(1969)**.
[3] M.Fantini, A.Gorenstein; Sol.Energy Mater., **16**, 487 **(1987)**.
[4] M.S.Wu, H.H.Hiseh; Electrochim.Acta, **53**, 3427 **(2008)**.
[5] A.Kowal, S.N.Port, R.J.Nichols; Catal.Today, **38**, 483 **(1997)**.

[6] T.Baird, K.C.Campbell, P.J.Holliman, R.W.Hoyle, D.Stirling, B.P.Williams and M.Morris; J.Mater.Chem., **7**, 319 **(1997)**.
[7] F.Cavani, F.Trifiro, A.Vaccari; Catal.Today, **11**, 173 **(1991)**.
[8] D.Leevin, J.Y.Ying; Stud.Surf.Sci.Catal., **110**, 367 **(1997)**.
[9] B.Sheela, H.Gomathi, R.G.Prabhakara; J.Electroanal.Chem., **394**, 267 **(1995)**.
[10] M.Yoshio, Y.Todorov, K.Yamato, H.Noguchi, J.Itoh, M.Okada, T.Mouri; J.Power Sources, **74**, 46 **(1998)**.
[11] H.X.Yang, Q.F.Dong, X.H.Hu; J.Power Sources, **79**, 256 **(1999)**.
[12] C.B.Alcock, B.Z.Li, J.W.Fergus, L.Wang; Solid State Ionics, **39**, 53-56, **(1992)**.
[13] H.Kumagai, M.Matsumoto, K.O.Toyoda; J.Mater.Sci.Lett., **15**, 1081 **(1996)**.
[14] E.L.Miller, R.E.Rocheleau; J.Electrochem.Soc., **144**, 3072 **(1997)**.
[15] M.Chigane, M.Ishikawa; J.Chem.Soc., Faraday Trans., **88**, 2203 **(1992)**.
[16] P.Lunkenheimer, A.Loidl, C.R.Ottermann, K.Bange; Phys.Rev.B, **44**, 5927 **(1991)**.
[17] P.Tomczyk, G.Mordarski, J.Oblakowski; J.Electroanal.Chem., **53**, 177 **(1993)**.
[18] R.C.Makkus, K.Hemmes, J.H.W.De Wit; J.Electrochem.Soc., **141,** 3429 **(1994)**.
[19] C.L.Cronan, F.J.Micale, M.Topic, H.Leidheiser, A.C.Zettlemoyer; J.Colloid Interface Sci., **55**, 546 **(1976)**.
[20] F.Fievet and M.Figlarz; J.Catal., **39**, 350 **(1975)**.
[21] J.M.Boyer, B.Répetti, R.Garrigos, M.Meyer A.Bée; J.Metastable and Nanocrystal Mater., **22**, 1 **(2004)**.
[22] R.J.M.Fernandez, J.Morales, J.L.Tirado; J.Mater.Sci., **21**, 3668 **(1986)**.
[23] V.V.Bakovets, L.N.Trushnikova, I.V.Korolkov, V.V.Sokolov, I.P.Dolgovesova, T.D.Pivovarova; Russ.J.Gen.Chem., **79**, 356 **(2009)**.
[24] L.Dong, Y.Chu, W.Sun; Chem.A Europ.J., **14**, 5064 **(2008)**.
[25] D.B.Kuang, B.X.Lei, Y.P.Pan, X.Y.Yu, C.Y.Su; J Phys.Chem.C., **113**, 5508 **(2009)**.
[26] J.Zhu, Z.Gui, Y.Ding, Z.Wang, Y.Hu, M.Zou; J.Phys.Chem.C., **111**, 5622 **(2007)**.
[27] F.Jiao, A.H.Hill, A.Harrison, A.Berko, A.V.Chadwick, P.G.Bruce; J.Amer.Chem.Soc., **130**, 5262 **(2008)**.
[28] T.L.Lai, Y.L.Lai, J.W.Yu, Y.Y.Shu, C.B.Wang; Mater.Res.Bull., **44**, 2040 **(2009)**.
[29] F.Hazell and R.J.Irving; Chem.Soc, **6**, 669 **(1966)**.
[30] V.Logvinenko, V.Bakovets, L.Trushnikova; J.Therm.Anal.Cal., **107**, 983 **(2012)**.
[31] K.M.Abd El-Salaam, E.A.Hassan; Surface Technology, **11**, 55 **(l980)**.
[32] R.M.Gabr, A.N.El-Naimi, M.G.Al-Thani; Thermochim.Acta, **197**, 307 **(1992)**.
[33] J.Rouquerol; Thermochim.Acta, **144**, 209 **(1989)**.
[34] K.Nahdi, P.Llewellyn, F.Rouquerol, J.Rouquerol, N.K.Ariguib, M.T.Ayedi; Thermochim.Acta, **390**, 123 **(2002)**.
[35] K.Nahdi, F.Rouquerol, M.T.Ayadi; Solid State Sci., **11**, 1028 **(2009)**.
[36] K.Nahdi, M.Férid, M.T.Ayadi; J.Therm.Anal.Cal., **96**, 455-461 **(2009)**.
[37] K.Nahdi, M.Férid, M.T.Ayadi; Thermochim.Acta, **487**, 54-59 **(2009)**.
[38] A.K.Galwey; Thermochimi.Acta, **355**, 181-238 **(2000)**.
[39] J.M.Criado, Perez L.A.Maqueda; in "Sample controlled thermal analysis: Origin, Goals, Multiple Forms, Applications and Future", Edited by Sorensen O.T.and Rouquerol J.Kluwer Acad.Publishers, Dordrecht, **(2003)**.
[40] J.H.Sharp, G.W, Brindley, B.N.N.Achar; J.Am.Ceram.Soc., **49**, 379 **(1966)**.
[41] J.M.Criado, A.Ortega, F.Gotor; Thermochim.Acta, **157**, 171 **(1990)**.
[42] A.Ortega, S.Akhouayri, F.Rouquerol, J.Rouquerol; Thermochim.Acta, **163**, 25 **(1990)**.